Shear flow instability in nematic liquids : theory steady simple shear flows

P. Manneville, E. Dubois-Violette

Classification
Physics Abstracts
6.300 — 7.130

SHEAR FLOW INSTABILITY IN NEMATIC LIQUIDS : THEORY STEADY SIMPLE SHEAR FLOWS

P. MANNEVILLE and E. DUBOIS-VIOLETTE (*)

Service de Physique du Solide et de Résonance Magnétique
Centre d'Etudes Nucléaires de Saclay, BP 2, 91190 Gif-sur-Yvette, France

(*Reçu le 20 octobre 1975, accepté le 19 décembre 1975*)

Résumé. — Nous étudions des instabilités de cisaillement dans un liquide nématique en géométrie *planaire* (molécules parallèles aux surfaces de l'échantillon) et où l'alignement des molécules (suivant Ox) est perpendiculaire à l'écoulement (suivant Oy). Un champ magnétique extérieur renforce l'alignement imposé par les effets de surface.

Nous développons un modèle bidimensionnel qui tient compte exactement des conditions aux limites sur le directeur et sur la vitesse de l'écoulement. Les deux types d'instabilité observés expérimentalement par Guyon et Pieranski (distorsion homogène et rouleaux convectifs parallèles à Oy) sont interprétés dans le cadre de ce modèle. On obtient les seuils d'instabilité ainsi que la valeur du vecteur d'onde critique q_x^c au seuil. En champ faible une distorsion homogène ($q_x^c = 0$) apparaît. Par contre en champ élevé, il se développe une instabilité en rouleaux ($q_x^c \neq 0$). On prévoit le changement de comportement pour un champ magnétique $H \simeq 1$ kG. On montre en outre que dans chaque cas, en ce qui concerne le directeur, l'allure de la distorsion selon Oz, est dominée par un seul mode q_z. Contrairement au cas de la distorsion homogène où q_z varie fortement avec H, pour l'instabilité en rouleaux, q_z reste voisin de $\pi/2\,a$ ($2\,a$: épaisseur de l'échantillon) ce qui permet de développer un calcul approché qui donne des résultats en bon accord avec ceux du calcul exact.

Abstract. — We study shear flow instabilities in nematic liquids of *planar* geometry (molecules parallel to the plates limiting the sample) and where molecules are aligned (along Ox) perpendicular to the shear flow direction (along Oy). An external magnetic field reinforces the alignement imposed by surface effects.

We develop a bidimensional model which takes into account exactly boundary conditions on the director and the velocity fields. The two types of instability which have been observed by Guyon and Pieranski (homogeneous distortion and convective rolls parallel to Oy) are interpreted within the framework of this model. We obtain instability thresholds together with the value of the critical wave vector q_x^c at threshold. Under weak fields the homogeneous distortion ($q_x^c = 0$) is achieved, whereas in high fields a roll instability develops ($q_x^c \neq 0$). The crossover from one regime to the other takes place at $H \simeq 1$ kG. Moreover, we show that in either case, as far as the director is concerned, the aspect of the distortion along the z-direction is dominated by only one wave vector q_z. Contrary to the case of the homogeneous distortion where q_z varies strongly with H, for the roll instability q_z remains nearly constant and close to $\pi/2\,a$ ($2\,a$ is the thickness of the sample). This allows us to develop an approximation which leads to results in good agreement with those obtained exactly.

1. **Introduction.** — In Nematic Liquid Crystals (N.L.C.), the coupling between the velocity field and the internal degree of freedom — the *director* field — leads to novel instability mechanisms when compared to isotropic liquids [1]. In particular, elementary flows such as simple shear flow or Poiseuille flow, in conveniently aligned N.L.C., may become unstable for very low Reynolds numbers. Moreover, due to the strong birefringence of the liquid crystals, the onset of an instability may be observed with high resolution by means of an optical detection of the alignment perturbation. All this makes the study of hydrodynamic instabilities in N.L.C. particularly attractive.

Let us consider a simple shear flow experiment in the geometry defined in figure 1 where :

— the fluid is enclosed between two parallel plates, one moving relative to the other in the y-direction and inducing a constant shear rate s in the bulk,

— molecules are aligned (through surface treat-

(*) Laboratoire de Physique des Solides, Université de Paris Sud, 91405 Orsay, France.

ment) in the x-direction (*planar* configuration with molecules perpendicular to the velocity of the plates),

— an external magnetic field parallel to Ox can be applied, reinforcing the alignment.

At low shears, the flow configuration is stable. However, when the shear rate s is increased above a critical value s_c the flow becomes distorted and one can observe different situations depending on the intensity of the applied magnetic field [2, 3] :

a) under weak fields a distortion of the director (uniform in the plane of the sample) appears at a certain threshold s_c. Following Pieranski and Guyon[3] we call this a homogeneous distortion (H.D.) ;

b) under strong fields (typically 3 kG) a convective motion develops at the threshold and one observes a pattern of rolls (axis parallel to Oy) strongly reminiscent of the Williams domains which appear in electrohydrodynamic instabilities [4].

In this paper we give a theoretical analysis of the steady shear flow experiments described by Guyon and Pieranski [2, 3], leaving to subsequent papers the case of alternating shear flow [3] and Poiseuille flow [5].

We work within the framework of a linear stability theory [6] and develop an analysis in terms of *normal modes* of the general form $\exp i(q_x x + q_z z)$ which correspond to the rolls experimentally observed. Before beginning detailed calculations we describe the mechanisms which lead to the two different instabilities by considering only particular modes such as $\cos(q_z z)$ or $\cos(q_x x)$, which leads to an adequate insight of the phenomena. The H.D., which may appear as the limiting case of a zero wave vector, is indeed a special case and will be examined first since it is much simpler. As in the case of electrohydrodynamical [7, 8] or thermal [9] instabilities, the complete bidimensional problem can only be solved numerically. Together with the critical shear rate, we obtain the wave vector of the most unstable mode (either zero or non zero) and compare our results with the experimental ones. A complete derivation of the linearized equations will be found in appendix A.

2. **Linearized hydrodynamic equations.** — Let us consider a very long and wide channel of thickness $2a$ and take the origin of coordinates midway between the two plates (Fig. 1). In order to stabilize the director field in the x-y plane, one applies a high (in order to avoid electrohydrodynamic instabilities [10]) frequency a.c. electric field in the z-direction ($\varepsilon_a < 0$). Moreover we assume strong anchoring conditions on the boundaries so that the alignment is kept rigidly fixed (parallel to Ox) at the plates. In the unperturbed state (denoted as ^{0}) this alignment prevails in the bulk and the velocity field is $v_x^0 = v_z^0 = 0$, $v_y^0 = sz$ where s is the shear rate ($s = v/2a$, v is the velocity of the upper plate relative to the lower one).

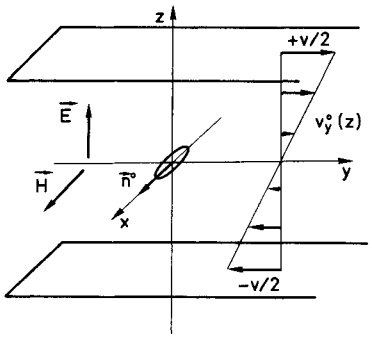

FIG. 1. — Geometry : A shear flow $v_y^0(z)$ is applied on a planar nematic (molecules along Ox).

Let us call the orientation fluctuation $\mathbf{n} = (0, n_y, n_z)$, the velocity fluctuation $\mathbf{v} = (v_x, v_y, v_z)$ and the pressure fluctuation p. The equations coupling these fluctuations are derived from the Ericksen-Leslie-Parodi formulation [11] and are given in appendix A. We shall restrict our attention to the case of solutions which are uniform in the flow direction (all quantities depend only on x and z).

2.1 TORQUE EQUATIONS. — The total torque Γ^t (viscous torque + elastic torque + torque induced by external fields) exerted on the molecules reads :

$$\Gamma_y^t = 0 = [\gamma_1 \partial_t n_z + \alpha_3 \partial_z v_x + \alpha_2 \partial_x v_z + \alpha_3 s n_y] + [-(K_1 \partial_{zz}^2 + K_3 \partial_{xx}^2) n_z] + \left[\left(\chi_a H^2 - \frac{\varepsilon_a}{4\pi} E^2\right) n_z\right] \quad (2.1)$$

$$\Gamma_z^t = 0 = [-\gamma_1 \partial_t n_y - \alpha_2 \partial_x v_y - \alpha_2 s n_z] + [(K_2 \partial_{zz}^2 + K_3 \partial_{xx}^2) n_y] + [-\chi_a H^2 n_y]. \quad (2.2)$$

If one considers modes such that $\mathbf{n} \sim \cos(q_x x)$, one sees that the elastic torques are stabilizing ($\Gamma_z < 0, \Gamma_y > 0$, Fig. 2). This is also the case of the magnetic torque and of the electric torque if $\varepsilon_a < 0$. The analysis of the viscous contribution will be given in the next section.

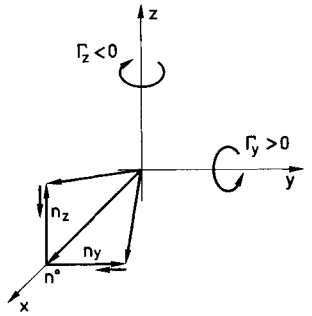

FIG. 2. — Stabilizing torques correspond to $\Gamma_z < 0$ or $\Gamma_y > 0$.

2.2 FORCE EQUATIONS. — The force equations given in appendix A may be simplified as follows :

— Inertial terms $\rho \partial_t v_\alpha$ may be neglected compared to viscous terms $\eta \partial_{\beta\gamma}^2 v_\alpha$ since the time scale associated

with the diffusion of velocity ($t_v = \rho a^2/\eta$) is much smaller than that associated with the diffusion of orientation ($t_0 = \gamma a^2/K$) which corresponds to the motions of interest (typical values for MBBA lead to $t_v \sim 10^{-3}$-10^{-4} s and $t_0 \sim 10^1$-10^2 s with $a = 10^{-2}$ cm, K $\sim 10^{-6}$ CGS, $\eta \sim \gamma \sim$ 0.1-1. CGS and $\rho = 1$ g/cm^3) [12].

— The same argument holds for the convective term $\rho s v_z$ as long as we are concerned with a low shear rate s.

— All terms containing the derivative ∂_y drop out since we consider uniform solutions in the y-direction.

Thus the force equations and the continuity equation read :

$$0 = -\partial_x p + (b\,\partial_{xx}^2 + \eta_1\,\partial_{zz}^2)\,v_x + (\eta_1 - \eta_3)\,s\,\partial_z n_y + \alpha_3\,\partial_{zt}^2 n_z \quad (2.3)$$

$$\rho s v_z = (\eta_2\,\partial_{xx}^2 + \eta_3\,\partial_{zz}^2)\,v_y + (\eta_2 - \eta_3)\,s\,\partial_x n_z + \alpha_2\,\partial_{xt}^2 n_y \quad (2.4)$$

$$0 = -\partial_z p + (\eta_2\,\partial_{xx}^2 + d\,\partial_{zz}^2)\,v_z + (\eta_3 - d)\,s\,\partial_x n_y + \alpha_2\,\partial_{xt}^2 n_z \quad (2.5)$$

with

$$d = \eta_3 - (\alpha_5 + \alpha_2)/2$$

$$0 = \partial_x v_x + \partial_z v_z\,. \quad (2.6)$$

Before performing a detailed analysis of eq. (2.1)-(2.6) let us examine how the unperturbed flow may become unstable against a fluctuation.

3. **Instability mechanisms.** — As we may consider that the velocity field responds instantly to an orientation fluctuation which, in contrast, decays much more slowly, we shall concentrate on the effect of an orientation fluctuation on the flow and discuss everything in terms of torques exerted on the molecules.

3.1 THE GUYON-PIERANSKI MECHANISM FOR A H.D. [3]. — Suppose a fluctuation $n_z > 0$. The flow exerts a viscous torque on the molecules proportional to n_z : $\Gamma_z = -\alpha_2\,s n_z$ which is positive since $\alpha_2 < 0$ [13] (Fig. 3*a*). This torque will make the molecules rotate

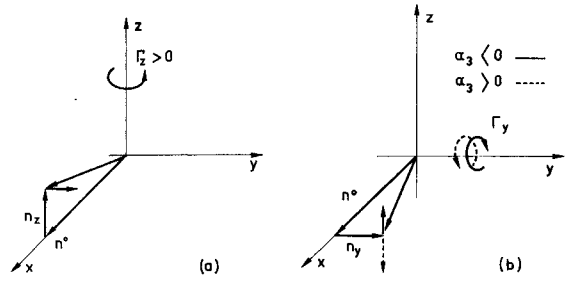

FIG. 3. — Guyon-Pieranski mechanism for a homogeneous distortion. *a*) Suppose a fluctuation $n_z > 0$. The flow induces a viscous torque $\Gamma_z > 0$ such that a fluctuation $n_y > 0$ appears. *b*) Suppose a fluctuation $n_y > 0$. The flow induces a viscous torque Γ_y such that the initial fluctuation n_z is : — increased if $\alpha_3 < 0$ ($\Gamma_y < 0$), — damped if $\alpha_3 > 0$ ($\Gamma_y > 0$).

in such a way that a small desorientation $n_y > 0$ is created. As a result of this fluctuation n_y, the flow exerts a viscous torque $\Gamma_y = \alpha_3\,s n_y$ on the molecules. This torque has the sign of α_3 (Fig. 3*b*). If $\alpha_3 < 0$, the viscous torque $\Gamma_y < 0$ induces a rotation of the molecules such that the initial fluctuation is increased ($n_z > 0$) : this leads to an instability (case of MBBA [2]). On the other hand if $\alpha_3 > 0$ the initial fluctuation is damped and the system is stable against this mechanism (case of HBAB at 80 °C [13]). In fact these destabilizing viscous torques have to overcome stabilizing elastic or field induced torques. The instability sets up when the shear rate is high enough for the balance to be reached. This completes the original version of the mechanism [3]. However the actual picture is slightly more complex due to the coupling between velocity and orientation. The distortion cannot be uniform in the z-direction since the boundary conditions can be satisfied only if some *twist* and *splay* appears in the bulk. The twist distortion induces shear flows which in turn create viscous torques. Let us examine how this effect modifies the mechanism.

Consider a distortion of the form $n_y \sim \cos(q_z z)$ (Fig. 4). This distortion induces an orientational viscous force $(\eta_1 - \eta_3)\,s\,\partial_z n_y$ (eq. (2.3)) which, due to

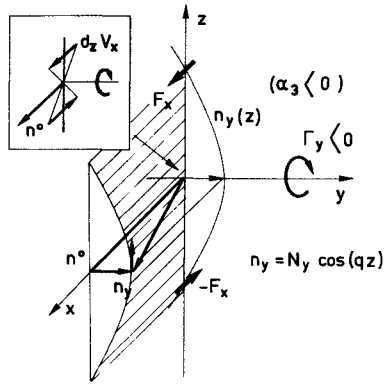

FIG. 4. — A twist distortion induces a viscous force F_x and then a shear flow as described on the insert. The resulting viscous torque depends on the sign of α_3 as in figure 3*b*.

the instantaneous response of the velocity field, is counterbalanced by a viscous force $\eta_1\,\partial_{zz}^2 v_x$. The initial fluctuation then creates a shear flow :

$$\partial_z v_x = \left(\frac{\eta_3}{\eta_1} - 1\right) s n_y\,.$$

This shear flow induces a torque component $\alpha_3\,\partial_z v_x$ which adds to the first term $\alpha_3\,s n_y$ to give an effective torque :

$$\Gamma_y = \alpha_3 \frac{\eta_3}{\eta_1}\,s n_y\,. \quad (3.1)$$

In general $\eta_3 > \eta_1$ so that the destabilizing mechanism is strengthened by the coupling to v_x. In order to

estimate the threshold let us suppose that $n_z \sim \cos(q_z z)$ and take into account the presence of a transverse velocity only through the change $\alpha_3 \to \alpha_3 \eta_3/\eta_1$. The torque equations lead to a compatibility condition which reads :

$$\left(K_1 q_z^2 + \chi_a H^2 - \frac{\varepsilon_a}{4\pi} E^2\right).(K_2 q_z^2 + \chi_a H^2) = = s^2 \alpha_2 \alpha_3 \eta_3/\eta_1 . \quad (3.2)$$

If one introduces approximate boundary conditions on n_y and n_z through the condition $q_z \sim \pi/2\, a$, the threshold is given at zero external field by

$$\left(\frac{\pi}{2}\right)^2 = sa^2 \sqrt{\frac{\alpha_2 \alpha_3}{K_1 K_2} \cdot \frac{\eta_3}{\eta_1}} \quad (3.3)$$

where the right-hand side has the form expected for an Ericksen number as defined in note [12].

Formally, the described mechanism works provided $\alpha_3 < 0$. However in the case where $\alpha_3 > 0$ or in presence of strong stabilizing external fields, new mechanisms related to a non-uniform distortion can induce new instabilities.

3.2 ROLL INSTABILITY. — The mechanism involves shear flows and viscous torques induced by a non-uniform distortion (*bend*) of the director. Consider for example a fluctuation $n_y \sim \cos(q_x x)$ (Fig. 5*a*).

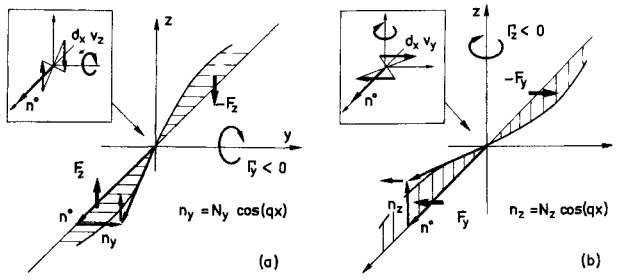

FIG. 5. — Mechanisms for a roll instability : *a*) a bend distortion $n_y(x)$ induces a shear flow in the z-direction which in turn induces a destabilizing viscous torque Γ_y ; *b*) a bend distortion $n_z(x)$ induces a shear flow in the y-direction such that the viscous torque $\Gamma_z < 0$ is stabilizing. The presence of an instability results from a complex interplay between mechanisms described in figures 3, 4, 5.

This bend distortion creates a *focalizing* force $(\eta_3 - d)\, s\, \partial_x n_y$ (eq. (2.5)) which is instantaneously counterbalanced by a viscous force $\eta_2\, \partial_{xx}^2 v_z$ and a shear flow

$$\partial_x v_z = \frac{d - \eta_3}{\eta_2} s n_y$$

is created. In addition to the viscous torque $\Gamma_y = \alpha_3\, s n_y$ described in 3.1, this shear flow gives a destabilizing contribution :

$$\alpha_2 \frac{d - \eta_3}{\eta_2} s n_y \quad (3.4)$$

to the total viscous torque Γ_y^v for $d > \eta_3$ (which is generally the case). This analysis indicates only how this new contribution may induce an instability. In fact the true mechanism is much more intricate. Indeed the *bend* distortion $n_z(x)$ (Fig. 5*b*) also creates a *focalizing* force which gives rise to a stabilizing contribution :

$$\alpha_2 \left(1 - \frac{\eta_3}{\eta_2}\right) s n_z \quad (3.5)$$

to the viscous torque Γ_z^v. Finally one has to take into account the effects of the *twist* distortion $n_y(z)$ as described in 3.1 which also induces a Γ_z^v contribution. As a result the different contributions to the viscous part of the torque equations are not independent of the wavelength of the distortion, as one might infer from eq. (3.1), (3.4), (3.5). The correct expressions for the effective torque equations will be developed further, together with an estimate of the threshold analogous to eq. (3.2). We now turn to the exact calculation and begin with the simpler case of the H.D.

4. **Homogeneous distortion.** — Suppose a fluctuation which is a function of z only. Then from boundary conditions and from eq. (2.4)-(2.6) we deduce : $v_z = \text{const.} = 0$, $v_y = \alpha z + \beta = 0$ and $p = 0$. Therefore, we are left with the problem of solving eq. (2.1)-(2.3). Let us look for solutions of the form :

$$n_{y(\text{or } z)}(z, t) = n_{y(\text{or } z)}(z) \exp i\omega t$$
$$v_x(z, t) = v_x(z) \exp i\omega t .$$

Performing the following transformation :

$$t = \frac{\gamma_1 a^2}{K_1} \bar{t} \quad \text{or} \quad \omega = \frac{K_1}{\gamma_1 a^2} \bar{\omega}$$
$$\bar{n}_y = \bar{n}_y, \bar{n}_z = \sqrt{|\, K_2 \alpha_3 / K_1 \alpha_2 \,|}\, \bar{n}_z$$

and

$$v_x = \frac{1}{a} \sqrt{|\, K_1 K_2 / \alpha_2 \alpha_3 \,|}\, \bar{v}_x$$
$$x = a\bar{x}, z = a\bar{z}, q_x = \bar{q}_x/a, q_z = \bar{q}_z/a$$

(for simplicity we shall omit the bar over all spatial quantities $\bar{x}, \bar{z}, \bar{q}_x, \bar{q}_z$ in the following) one obtains the dimensionless equations :

$$(-D^2 + F + i\bar{\omega})\, \bar{n}_z + \sigma D \bar{v}_x + \sigma E_r \bar{n}_y = 0 \quad (4.1)$$
$$(-D^2 + G + ik\bar{\omega})\, \bar{n}_y - E_r \bar{n}_z = 0 \quad (4.2)$$
$$D^2 \bar{v}_x + i\bar{\omega}\sigma\varepsilon D \bar{n}_z + (1 - e)\, E_r D \bar{n}_y = 0 \quad (4.3)$$

with

$$D = \partial_z, k = K_1/K_2, \varepsilon = \alpha_3^2/\gamma_1 \eta_1, e = \eta_3/\eta_1, \quad \sigma = \alpha_3/|\, \alpha_3 \,|$$

and

$$E_r = sa^2 \sqrt{|\, \alpha_2 \alpha_3 / K_1 K_2 \,|} \quad (4.4)$$

$$F = \left(\chi_a H^2 - \frac{\varepsilon_a}{4\pi} E^2\right) \frac{a^2}{K_1} \quad \text{and} \quad G = \chi_a H^2 \frac{a^2}{K_2} .$$

E_r is the Ericksen number [12] characterizing the flow and F and G are dimensionless parameters which measure the intensity of external fields. In appendix B we show that (except for very pathological flows) the instability is *stationnary* : the principle of exchange of stabilities [6] is valid and $\omega = 0$ at threshold. Then the system (4.1)-(4.3) reduces to

$$D(D^4 - (F + G) D^2 + \sigma E'^2 + FG) \bar{n}_y = 0 \quad (4.5)$$

where $E'^2 = eE_r^2$. Solving this equation one obtains :

$$\bar{n}_y = \sum_{\pm} A_{\pm} \cos(q_{\pm} z) + B_{\pm} \sin(q_{\pm} z) + C$$

where $q_{\pm} = \sqrt{p_{\pm}}$ and $p_{\pm}$ are the two roots of the characteristic equation :

$$\left.\begin{aligned} &p^2 + (F + G) p + FG + \sigma E'^2 = 0 \\ &p_{\pm} = \tfrac{1}{2}[-(F + G) \pm \sqrt{(F - G)^2 - 4\sigma E'^2}] \end{aligned}\right\} \quad (4.6)$$

$\bar{n}_z$ is deduced from eq. (4.2) :

$$E_r \bar{n}_z = \sum_{\pm} (p_{\pm} + G)(A_{\pm} \cos q_{\pm} z + B_{\pm} \sin q_{\pm} z) + GC$$

and from eq. (4.1), (4.2) one obtains :

$$E_r \bar{v}_x = \sum_{\pm} f_{\pm}(A_{\pm} \sin q_{\pm} z - B_{\pm} \cos q_{\pm} z) - Cgz + C'$$

with $f_{\pm} = E_r^2(e - 1)/q_{\pm}$ and $g = E_r^2 + \sigma FG$.

The solution $(\bar{n}_y, \bar{n}_z, \bar{v}_x)$ has to satisfy the boundary conditions $\bar{n}_y = \bar{n}_z = \bar{v}_x = 0$ at $z = \pm 1$.

This gives a system of six homogeneous equations with 6 unknowns $A_{\pm}$, $B_{\pm}$, C, C' which may be split into two decoupled sets :

System A

$$\left.\begin{aligned} &\sum_{\pm} A_{\pm} \cos q_{\pm} + C = 0 \\ &\sum_{\pm} A_{\pm} p_{\pm} \cos q_{\pm} = 0 \\ &\sum_{\pm} A_{\pm} f_{\pm} \sin q_{\pm} - Cg = 0 \end{aligned}\right\} \quad (4.7)$$

corresponds to a solution where the distortion $(\bar{n}_y, \bar{n}_z)$ is an even function of z and leads to the compatibility condition :

$$p_+ \cos q_+(f_- \sin q_- + g \cos q_-) = p_- \cos q_-(f_+ \sin q_+ + g \cos q_+) . \quad (4.8)$$

System B

$$\left.\begin{aligned} &\sum_{\pm} B_{\pm} \sin q_{\pm} = 0 \\ &\sum_{\pm} B_{\pm} p_{\pm} \sin q_{\pm} = 0 \\ &\sum_{\pm} B_{\pm} f_{\pm} \cos q_{\pm} - C' = 0 \end{aligned}\right.$$

corresponds to a distortion $(\bar{n}_y, \bar{n}_z)$ which is an odd function of z. It leads to :

$$\sin q_+ \sin q_-(p_- - p_+) = 0$$

or

$$E'^2 = (F + (\lambda\pi)^2)(G + (\lambda\pi)^2)$$

where λ is some integer. The solution is then :

$$\bar{n}_y = N \sin(\lambda\pi z)$$
$$E_r \bar{n}_z = ((\lambda\pi)^2 + G) N \sin(\lambda\pi z)$$
$$\bar{v}_x = -\frac{E_r}{\lambda\pi}(e - 1) N(\cos(\lambda\pi z) - (-1)^{\lambda}) .$$

However such a solution which corresponds to a uniform distortion in the $(x - y)$ plane cannot be retained in order to interpret experiments with a channel of finite width since then a net flow :

$$\int_{-1}^{+1} v_x(z)\, dz = 2(-1)^{\lambda} \frac{E_r(e - 1)}{\lambda\pi} N \neq 0$$

would take place in the transverse direction, which cannot be sustained all along the sample. On the other hand the solution v_x of system A is an odd function of z and

$$\int_{-1}^{+1} v_x(z)\, dz = 0$$

there exists a convective roll inside the sample which is allowed to close in boundary layers on each side of the experimental cell. Let us now look for numerical solutions of system A.

Here we consider only the case $\alpha_3 < 0$ ($\sigma = -1$) where the mechanism described in section 2.1 is destabilizing. Moreover we suppose that the electric and magnetic fields are both stabilizing ($\varepsilon_a < 0$, F and G positive). Numerical calculations have been performed with values of physical constants given in table I relative to MBBA at 25 °C. Eq. (4.6) defines the relation between the modes $q_{\pm}$ and the applied shear s. For a fixed shear, the solution has to satisfy boundary conditions (4.7), which leads to an implicit eq. (4.8) of the form $f(s) = 0$. The treshold corresponds to the first (non-trivial [15]) solution of this equation. It is plotted as a function of the magnetic

TABLE I

MBBA 25 °C (CGS units)

$\eta_1 = 0.238$	$\eta_2 = 1.035$	$\eta_3 = 0.416$	[13a]
$\alpha_1 = 0.065$	$\alpha_2 = -0.785$	$\alpha_3 = -0.012$	
$b = 0.756$	$d = 0.582$		
$K_1 = 6 \times 10^{-7}$	$K_2 = 3 \times 10^{-7}$	$K_3 = 7 \times 10^{-7}$	[11]
$\rho = 1.088$			[11b]
$\varepsilon_{\parallel} = 4.71$	$\varepsilon_{\perp} = 5.26$	$\frac{\varepsilon_a}{4\pi} = -0.0438$	[16]
$\chi_{\parallel} = 5.80 \times 10^{-7}$	$\chi_{\perp} = 4.66 \times 10^{-7}$	$\chi_a = 1.14 \times 10^{-7}$	[17]

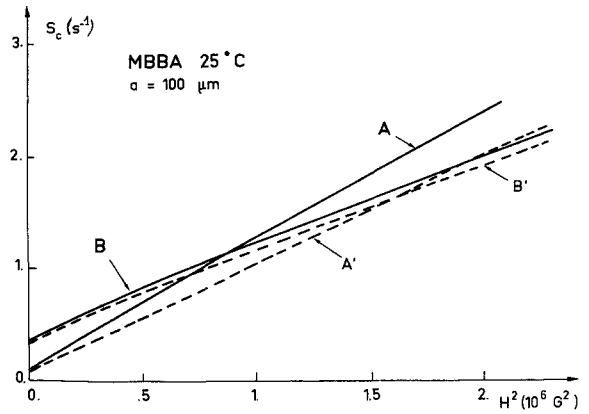

FIG. 6. — Instability threshold s_c as a function of the magnetic field. 1) Homogeneous distortion : — Curve A corresponds to the calculation taking into account the whole set of boundary conditions. — Curve A' corresponds to the one mode approximation with $q_z = \pi/2$. 2) Roll instability : — Curve B corresponds to the exact calculation. — Curve B' displays the approximate threshold as given by the minimum of $s(q_x, q_z)$ for $q_z = \pi/2$.

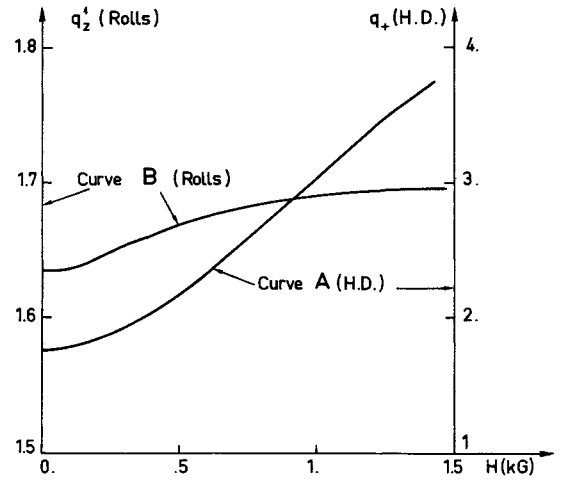

FIG. 7. — Variation of the *dominant* z-wave vector as a function of the magnetic field. Curve A corresponds to the homogeneous distortion (scale on the right) and curve B to the roll instability (left scale); q_+ and q_z^1 are the *dominant* wave vectors given in table I and II.

field in figure 6 curve A. Curve A' represents the threshold curve obtained from the estimate 3.2 where one has taken into account boundary conditions by imposing $q_z = \pi/2$. The discrepancy, which increases with the magnetic field, between the exact and approximate results is due to the fact that for the approximate curve one neglects the boundary condition on v_x. In fact taking $n_y \sim \cos(q_z z)$ leads to

$$v_x \sim \sin(q_z z) + \text{const.}$$

(eq. (4.1)) and $v_x \neq 0$ for $z = \pm 1$. On the other hand the exact solution is a superposition of several modes and fits all boundary conditions. The most striking feature of this solution is the fact that one mode dominates the other one and gives the solution its aspect, as far as the director is concerned. The calculation shows :

— that the real wave vector q_+ has an amplitude A_+ much greater than A_- corresponding to q_- which is purely imaginary,

— that A_-/A_+ decreases rapidly while q_+ and q_- grow slowly when the field is increased.

Comparison is made in table II and the growth of the dominant wave vector q_+ is given in figure 7 curve A. Profiles of n_y, n_z and v_x for $H = 0$ and $H = 1\,400$ G given in figure 8*a*, *b* illustrate the dominant role and the increase of q_+.

TABLE II

H (kG)	q_+	$-iq_-$	$-A_-/A_+$
0	1.75	1.75	5.9×10^{-2}
1.4	3.70	11.63	1.5×10^{-6}

Comparison with experimental results is rather difficult due to the relatively poor knowledge of the

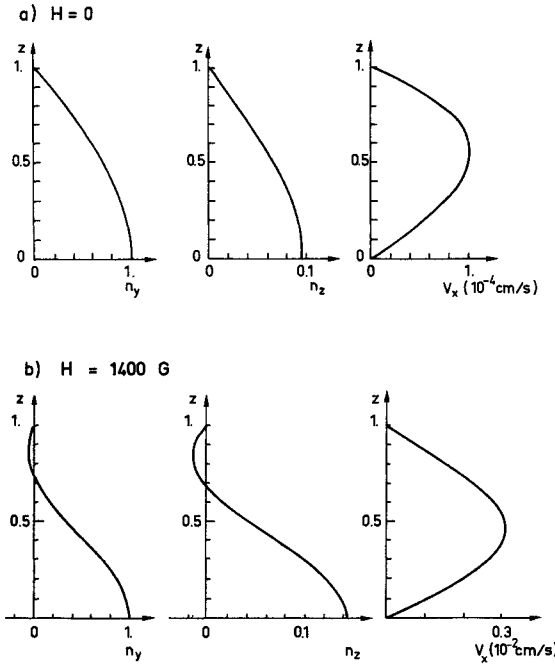

FIG. 8. — Fluctuation profiles for the homogeneous distortion : *a*) for $H = 0$; *b*) for $H = 1\,400$ G.

actual viscoelastic constants of the material which are sensitive to temperature changes, impurities and even the age of the sample (see the dispersion of numerical values tabulated in reference [11a]). However, from eq. (4.8) at zero applied field recalling the definition (4.4) we get :

$$E_r = 2.309$$

which corresponds to a critical velocity

$$v_c = 2\,a s_c = 2 \times 10^{-3}\ \text{cm/s}$$

for a sample of thickness 0.2 mm. This is in qualitative agreement with the value of 1.15×10^{-3} cm/s reported in reference [2]. To conclude this section let us point out that the existence of a transverse velocity has just been checked experimentally.

5. **Roll instability.** — As shown in section 3, a fluctuation of orientation which is space dependent in the x-direction can trigger the instability. The stability of the system is analysed by considering fluctuation *normal modes* of the form :

$$w_\alpha(x, z, t) = w_\alpha \exp i(q_x x + q_z z + \omega t)$$

where w_α stands for $n_y, n_z, v_x, \ldots, p$. In agreement with experimental results, we suppose moreover that the instability is stationnary so that ω is purely imaginary; then the threshold is reached for $\omega = 0$. As in 4 all lengths are scaled to a, but now all other variables keep their dimensional character. Let us introduce the following notation :

$$\begin{aligned}
f_z &= K_1 q_z^2 + K_3 q_x^2 + \left(\chi_a H^2 - \frac{\varepsilon_a}{4\pi} E^2\right) a^2 \\
f_y &= K_2 q_z^2 + K_3 q_x^2 + \chi_a H^2 a^2 \\
\beta_1 &= b q_x^2 + \eta_1 q_z^2 \\
\beta_2 &= \eta_2 q_x^2 + \eta_3 q_z^2 \\
\beta_3 &= \eta_2 q_x^2 + d q_z^2 \\
f &= \beta_1 q_z^2 + \beta_3 q_x^2 \\
\mu &= (\eta_3 - d) q_x^2 + (\eta_3 - \eta_1) q_z^2 .
\end{aligned}$$

The system (2.1)-(2.6) now becomes a linear homogeneous set of equations :

$$f_z n_z + \alpha_3 s a^2 n_y + \alpha_3 i q_z a v_x + \alpha_2 i q_x a v_z = 0 \quad (5.1)$$

$$f_y n_y + \alpha_2 s a^2 n_z + \alpha_2 i q_x a v_y = 0 \quad (5.2)$$

$$- i q_x a p - \beta_1 v_x + i q_z a(\eta_1 - \eta_3) s n_y = 0 \quad (5.3)$$

$$- \rho s a^2 v_z - \beta_2 v_y + i q_x a(\eta_2 - \eta_3) s n_z = 0 \quad (5.4)$$

$$- i q_z a p - \beta_3 v_z + i q_x a(\eta_3 - d) s n_y = 0 \quad (5.5)$$

$$i q_x v_x + i q_z v_z = 0 . \quad (5.6)$$

Eliminating all variables except n_y and n_z, the torque eq. (5.1), (5.2) become :

$$f_z n_z + (\alpha_3 - \mu(\alpha_2 q_x^2 - \alpha_3 q_z^2)/f) s a^2 n_y = 0 \quad (5.7)$$

$$(f_y + \alpha_2 s^2 a^4 \rho q_x^2 \mu / f \beta_2) n_y + (\alpha_2 \eta_3 (q_x^2 + q_z^2)/\beta_2) s a^2 n_z = 0 \quad (5.8)$$

and yield the compatibility condition :

$$f_z(f_y f \beta_2 + \alpha_2 s^2 a^4 \rho q_x^2 \mu) = \alpha_2 \eta_3 (q_x^2 + q_z^2) \times \times (\alpha_3 f - \mu(\alpha_2 q_x^2 - \alpha_3 q_z^2)) s^2 a^4 . \quad (5.9)$$

We now sketch the procedure : under given fields (H, E) consider a particular shear rate s and a given wave vector q_x. Eq. (5.9), which is of fifth-order in q_z^2, defines ten roots (modes) $\{ \pm q_z^j, j = 1,5 \}$ in terms of s and q_x. The general solution of system (5.1)-(5.6) depends on ten arbitrary constants. This solution can be expressed in terms of one unknown, say w_α, as a superposition :

$$w_\alpha = \sum_{j=1}^{10} A_j \exp i(q_x x + q_z^j z) ,$$

all other fluctuations w_β being deduced from w_α. This general solution then has to satisfy boundary conditions :

$$n_y = n_z = v_x = v_y = v_z = 0 \quad \text{at} \quad z = \pm 1 .$$

The ten subsequent conditions lead to a homogeneous system of 10 equations for the 10 unknowns $\{ A_j, j = 1, 10 \}$. Generally if the shear rate s and the wave vector q_x are fixed at arbitrary values, no superposition of the ten modes other than the trivial one $(A_j = 0; j = 1,10)$ will satisfy the boundary conditions. However, q_x and s may be chosen in order to satisfy boundary conditions in a non-trivial way : defining therefore the instability curve $s(q_x)$. The threshold is then obtained for the minimum shear rate s_c and defines the critical wave vector q_x^c at threshold. Let us now be more explicit. To take advantage of the fact that boundary conditions are symmetrical relative to the origin and that the ten modes are opposite by pairs it is convenient to choose a superposition of sines and cosines instead of the exponentials. Suppose n_y given by :

$$n_y = \sum_{j=1}^{5} [A_j \cos q_z^j z + B_j \sin q_z^j z] \cos q_x x .$$

We then have :

$$v_z = - q_x s a \sum \mathcal{U}(q_z^j) \times \times [A_j \cos q_z^j z + B_j \sin q_z^j z] \sin q_x x$$

$$v_x = s a \sum q_z^j \mathcal{U}(q_z^j) [A_j \sin q_z^j z - B_j \cos q_z^j z] \cos q_x x$$

$$n_z = - s a^2 \sum \mathcal{N}(q_z^j) \times \times [A_j \cos q_z^j z + B_j \cos q_z^j z] \cos q_x x$$

$$v_y = q_x s^2 a^3 \sum \mathcal{W}(q_z^j) \times \times [A_j \cos q_z^j z + B_j \sin q_z^j z] \sin q_x x$$

where $\sum$ stands for $\sum_{j=1}^{5}$ and

$$\begin{aligned}
\mathcal{U}(q) &= \mu(q)/f(q) \\
\mathcal{N}(q) &= [\alpha_3 - (\alpha_2 q_x^2 - \alpha_3 q^2) \mathcal{U}(q)]/f_z(q) \\
\mathcal{W}(q) &= [\rho \mathcal{U}(q) + (\eta_2 - \eta_3) \mathcal{N}(q)]/\beta_2(q) .
\end{aligned}$$

As in the case of the homogeneous distortion, boundary conditions lead to two decoupled sets corresponding to solutions of different parity. The

system corresponding to n_y and n_z even functions of z reads :

$$\begin{aligned} &\sum A_j \cos q_z^j = 0 \\ &\sum A_j \mathcal{N}(q_z^j) \cos q_z^j = 0 \\ &\sum A_j \mathcal{U}(q_z^j) \cos q_z^j = 0 \\ &\sum A_j q_z^j \mathcal{U}(q_z^j) \sin q_z^j = 0 \\ &\sum A_j \mathcal{W}(q_z^j) \cos q_z^j = 0 \,. \end{aligned} \tag{5.10}$$

The one corresponding to n_y and n_z odd functions of z is obtained through the interchange of the sines and cosines. The system (5.10) will have a non-trivial solution only if the determinant of the linear system is zero. This leads to the required relation between s and q_x under given external fields. Since the analytical solution is not tractable we have developed a numerical computation which closely follows the procedure sketched above. Figures 9, 10 give examples of instability curves $s(q_x)$ for different magnetic fields. Figure 9, curve A, corresponds to $H=0$. It shows two minima : one at finite q_x (2.0) and $s = 0.36\ s^{-1}$ and another one at $q_x = 0$ and $s = 0.10\ s^{-1}$ which gives the threshold. Figure 10, curve A, corresponds to $H = 1\,400$ G. The threshold is obtained for $s = 1.98\ s^{-1}$ and $q_x = 3.35$. The point X which belongs to another nappe than curve A corresponds to the homogeneous distortion. Therefore at high magnetic fields a roll instability is preferred to the homogeneous one. The threshold as a function of the magnetic field is plotted in figure 6 curve B. The change from the H.D. (which takes place in low fields) to the rolls is given by the intersection of curve A and B. It occurs at $H = 940$ G. Profiles of n_y, n_z, v_x, v_y, v_z are given in figure 11 for $H = 1\,400$ G. The aspect of the rolls is more clearly illustrated in figure 12. Here again, as in the case of the homogeneous distortion, there is always a dominant wave vector q_z as indicated in table III. One sees in figure 7 that this dominant wave vector is nearly constant and of order $\pi/2$ as the magnetic field is

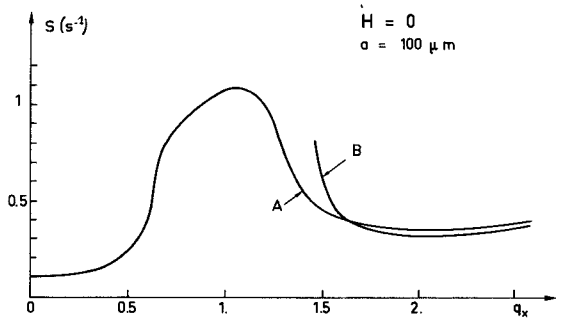

FIG. 9. — $H = 0$.

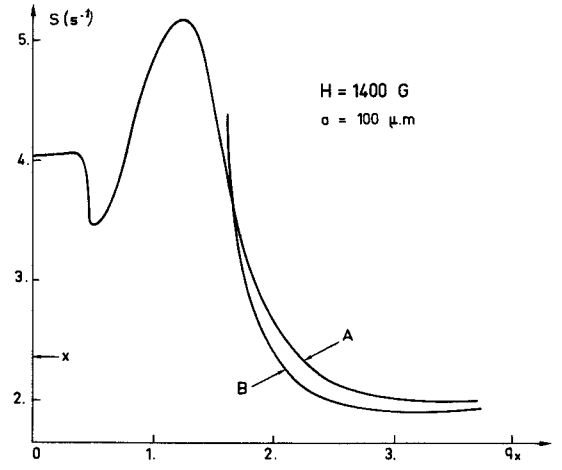

FIG. 10. — $H = 1\,400$ G.

FIG. 9-10. — Roll instability curves $s(q_x)$. Curves A correspond to the calculation taking into account the whole set of boundary conditions, curves B correspond to $s(q_x, q_z = \pi/2)$.

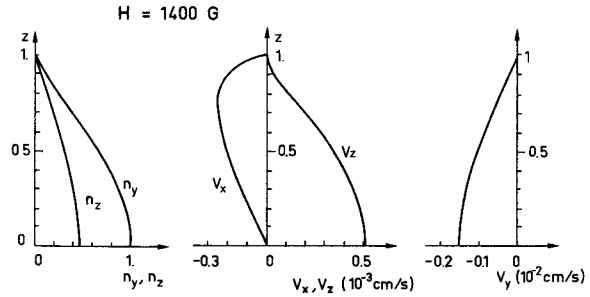

FIG. 11. — Fluctuation profiles for the roll instability.

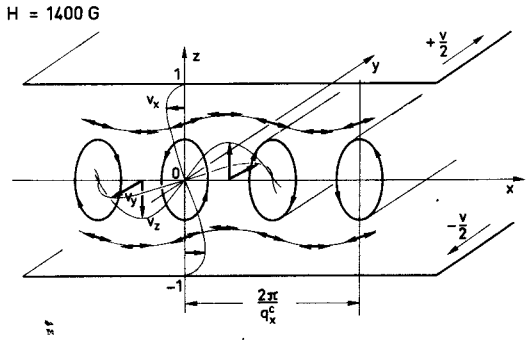

FIG. 12. — Flow pattern.

TABLE III

j	q_z^j	A_j
1	1.694 7	1
2	$i \times 14.19$	-4.73×10^{-8}
3	$6.0 - i \times 7.54$	$-(3.13 + i \times 6.48)\ 10^{-5}$
4	$6.0 + i \times 7.54$	$-(3.13 - i \times 6.48)\ 10^{-5}$
5	$i \times 3.36$	7.37×10^{-5}

increased. This allows to look for an approximate threshold value by the following approach : neglect the term containing ρ which comes from $\rho s v_z$ and impose $q_z = \pi/2$. Eq. (5.9) then reads :

$$s^2 a^4 = \frac{f_y f_z \beta_2}{\alpha_2 \eta_3 (q_x^2 + q_z^2)(\alpha_3 - \mu(\alpha_2 q_x^2 - \alpha_3 q_z^2)/f)}$$

and defines the instability curve $s(q_x, q_z = \pi/2)$ given in figure 9 and 10 curve B. This procedure (which is valid only for the roll instability, $q_x \gtrsim \pi/2$, since the homogeneous one does not correspond to a constant dominant wave vector q_z) gives quite good results for the threshold value (compare curve B and B' on figure 6) and even for the critical wave vector q_x^c at threshold (Fig. 13).

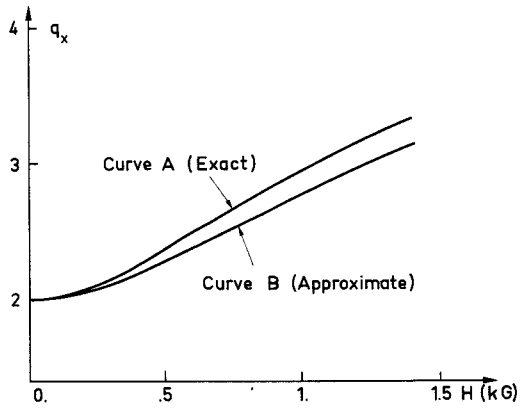

FIG. 13. — Critical wave-vector at the threshold as a function of the magnetic field. Curve A : exact calculation. Curve B : evaluation for a wave vector $q_z = \pi/2$.

The roll instability has been extensively studied in the case of alternating shear experiments [3]. For the static case, an experimental limitation comes from the maximum available relative displacement of the two horizontal plates limiting the channel and from the time required to set up the instability. Near the threshold this time becomes very long and may be much greater than the time necessary for the steady shear experiment itself. Such a drawback is absent in the case of a conventional Couette experiment where the liquid flows between two coaxial cylinders in relative rotation. Experiments by this method are under way ([1]) and provide a check of our theoretical results, particularly concerning the crossover from a H.D. to the convective rolls and the variation of the wavelength of the rolls as a function of the applied fields.

6. **Conclusion.** — This paper gives a study of steady simple shear flow instabilities resulting from a bidimensional analysis. We have considered only linear effects and moreover have assumed that the so called *Principle of Exchange of Stabilities* [6] holds for this problem. This point has only be proven in an approximate way for the case of the homogeneous distortion in Appendix B.

The mechanisms which lead to the instability are understood in terms of effective viscous torques as discussed first by Guyon and Pieranski [3] and reviewed in section 3 of this article. Their exact expression is given by eq. (5.7)-(5.8). An analysis in terms of a one dimensional model gives a good understanding of the instability mechanisms : the homogeneous instability is well described by modes with $q_x = 0$ and q_z given by boundary conditions. On the other hand the mechanism leading to rolls corresponds to finite q_x. But in this case in order to satisfy boundary conditions one also needs to introduce modes of finite q_z, which implies the bidimensional calculation : for MBBA at 25 °C the homogeneous distortion appears in presence of a magnetic field lower than about 1 kG ; otherwise rolls parallel to Oy are expected.

Beyond this particular result which is in qualitative agreement with available experimental observations, the exact calculation leads to an important and useful result :

Whereas the homogeneous distortion is sensitive to an exact fit of boundary conditions, the roll instability looks like a distortion which, as far as the director is concerned, may be characterized by a single mode $q_z \sim \pi/2$. Consequently the approximation $q_z = \pi/2$ in the effective torque eq. (5.7)-(5.8) will be very good. Moreover, the *natural* assumption of roughly circular rolls ($q_x \simeq q_z$) is not good : q_x and q_z are in some sense decoupled. Boundary conditions on the director field are easily satisfied by $q_z \simeq \pi/2$; q_x adjusts itself at an optimum value such that restoring torques equilibrate at best the destabilizing viscous torques.

These features deduced from the exact calculation will be of great use in the quantitative interpretation of forthcoming experiments as well as in the theory of alternating shear flow and Poiseuille flow instabilities which are presently in progress.

Acknowledgments. — The authors would like to thank P. G. de Gennes, E. Guyon, and P. Pieranski for very stimulating discussions.

([1]) Janossy, J., Guyon, E., Pieranski, P., private communication.

Appendix A. — We derive the set of equations coupling the director and velocity fluctuations keeping only first order terms in $n_y, n_z, v_x, v_y, v_z, p$

a) Torque equations :

The total torque exerted on the molecules is the sum of an elastic part Γ^e, plus a part due to external fields Γ^f, plus a part due to viscosity effects. The sum $\Gamma^1 = \Gamma^e + \Gamma^f$ can be derived from the free energy :

$$F = \int_V (\mathcal{F}^e + \mathcal{F}^f)\, d^3r .$$

The Frank elastic energy density $\mathcal{F}^e$ reads :

$$\mathcal{F}^e = \tfrac{1}{2}(K_1(\text{div } \mathbf{n})^2 + K_2(\mathbf{n}.\text{curl } \mathbf{n})^2 + K_3(\mathbf{n} \times \text{curl } \mathbf{n})^2)$$

and

$$\mathcal{F}^f = -\chi_a(\mathbf{n}.\mathbf{H})^2 - \frac{\varepsilon_a}{4\pi}(\mathbf{n}.\mathbf{E})^2$$

where $\chi_a = \chi_{\parallel} - \chi_{\perp}$ is positive for rod shaped molecules and $\varepsilon_a = \varepsilon_{\parallel} - \varepsilon_{\perp}$ may be positive (case of HBAB) or negative (case of MBBA). We have

$$\mathbf{\Gamma}^1 = \mathbf{n} \times \mathbf{h}$$

where the molecular field $\mathbf{h}$ reads

$$\mathbf{h} = -\delta F/\delta \mathbf{n}$$

($\delta/\delta\mathbf{n}$ denotes the functional derivative) ; up to first order we get :

$$\Gamma_x^1 = 0 .$$

$$\Gamma_y^1 = -h_z = -\left[\left(K_1\,\partial_{zz}^2 + K_2\,\partial_{yy}^2 + K_3\,\partial_{xx}^2 - \chi_a H^2 + \frac{\varepsilon_a}{4\pi}E^2\right) n_z + (K_1 - K_2)\,\partial_{yz}^2 n_y\right] \quad (A.1)$$

$$\Gamma_z^1 = h_y = (K_1\,\partial_{yy}^2 + K_2\,\partial_{zz}^2 + K_3\,\partial_{xx}^2 - \chi_a H^2)\, n_y + (K_1 - K_2)\,\partial_{yz}^2 n_z . \quad (A.2)$$

The viscous torque exerted by the flow on the molecules is given by the antisymmetric part of the Ericksen-Leslie stress tensor $\bar{\bar{\sigma}}'$. With implicit summation over indices which are repeated twice, its components read :

$$\sigma'_{ij} = \alpha_1(n_k A_{kl} n_l) n_i n_j + \alpha_2 n_i N_j + \alpha_3 N_i n_j + \alpha_4 A_{ij} + \alpha_5 n_i n_k A_{kj} + \alpha_6 A_{ik} n_k n_j$$

with

$$\mathbf{N} = \text{d}\mathbf{n}/\text{d}t - \tfrac{1}{2}(\text{curl } \mathbf{v}) \times \mathbf{n}$$

where

$$\text{d}/\text{d}t = \partial_t + \mathbf{v}.\nabla$$

and

$$A_{ij} = \tfrac{1}{2}(\partial_i v_j + \partial_j v_i) .$$

Then

$$\Gamma_i^v = \varepsilon_{ijk}\,\sigma'_{jk}$$

or

$$\mathbf{\Gamma}^v = -\mathbf{n} \times (\gamma_1 \mathbf{N} + \gamma_2 \mathbf{A}.\mathbf{n})$$

with

$$\gamma_1 = \alpha_3 - \alpha_2 \qquad \text{and} \qquad \gamma_2 = \alpha_3 + \alpha_2 .$$

Neglecting second order terms we get $\Gamma_x^v = 0$ and :

$$\Gamma_y^v = \gamma_1(\partial_t + v^0\,\partial_y)\, n_z + \alpha_3\,\partial_z v_x + \alpha_2\,\partial_x v_z + \alpha_3\, s n_y \quad (A.1')$$

$$\Gamma_z^v = -[\gamma_1(\partial_t + v^0\,\partial_y)\, n_y + \alpha_3\,\partial_y v_x + \alpha_2\,\partial_x v_y + \alpha_2\, s n_z] . \quad (A.2')$$

Angular momentum conservation leads to the torque balance equation

$$\mathbf{\Gamma}^t = \mathbf{\Gamma}^1 + \mathbf{\Gamma}^v = 0 .$$

b) Force equations :

Linear momentum conservation leads to the acceleration equations :

$$\rho \frac{\text{d}}{\text{d}t} v_i = -\delta_{ij}\,\partial_j p + \partial_j(\sigma_{ji}^e + \sigma'_{ji})$$

where the elastic stress tensor $\bar{\bar{\sigma}}^e$ given by

$$\sigma_{ij}^e = -(\partial\mathcal{F}^e/\partial(\partial_i n_k)).(\partial_j n_k)$$

does not contribute to first order.

One obtains :

$$\rho(\partial_t + v^0\,\partial_y)\,v_x = -\,\partial_x p + (b\,\partial_{xx}^2 + \eta_1(\partial_{yy}^2 + \partial_{zz}^2))\,v_x + \frac{\alpha_6 - \alpha_3}{2}\,s\,\partial_y n_z + \frac{\alpha_3 + \alpha_6}{2}\,s\,\partial_z n_y + \\ + \alpha_3[(\partial_t + v^0\,\partial_y)(\partial_y n_y + \partial_z n_z) + s\,\partial_y n_z] \quad (A.3)$$

$$\rho(\partial_t + v^0\,\partial_y)\,v_y + \rho s v_z = -\,\partial_y p + (\eta_2\,\partial_{xx}^2 + \eta_3(\partial_{yy}^2 + \partial_{zz}^2))\,v_y + \frac{\alpha_5 + \alpha_2}{2}\,\partial_{xy}^2 v_x + \frac{\alpha_5 - \alpha_2}{2}\,s\,\partial_x n_z + \\ + \alpha_2(\partial_t + v^0\,\partial_y)\,\partial_x n_y \quad (A.4)$$

$$\rho(\partial_t + v^0\,\partial_y)\,v_z = -\,\partial_z p + (\eta_2\,\partial_{xx}^2 + \eta_3(\partial_{yy}^2 + \partial_{zz}^2))\,v_z + \frac{\alpha_5 + \alpha_2}{2}\,\partial_{xz}^2 v_x + \frac{\alpha_5 + \alpha_2}{2}\,s\partial_x n_y + \\ + \alpha_2(\partial_t + v^0\,\partial_y)\,\partial_x n_z \quad (A.5)$$

with

$$\eta_1 = (\alpha_3 + \alpha_4 + \alpha_6)/2,\ \eta_2 = (\alpha_4 + \alpha_5 - \alpha_2)/2,\ \eta_3 = \alpha_4/2,\ b = \eta_1 + \alpha_1 + \alpha_5\,.$$

c) The continuity equation for an incompressible N.L.C. reads

$$\partial_x v_x + \partial_y v_y + \partial_z v_z = 0\,. \quad (A.6)$$

Appendix B. — In this appendix we discuss the character of the homogeneous instability either oscillatory or stationary. The derivation follows the one given for the Rayleigh-Bénard instability in reference [6]. Let us multiply eq. (4.1) by $E_r\,\bar{n}_y^*$ and integrate over the interval $[-1, +1]$. This gives :

$$\int dz\,\bar{n}_y^*(-D^2 + F + i\bar{\omega})\,E_r\,\bar{n}_z + \int dz\,\sigma E_r\,\bar{n}_y^*\,D\bar{v}_x + \sigma E_r^2 \int dz\,|\,\bar{n}_y\,|^2 = 0 \quad (B.1)$$

using eq. (4.2) we have to evaluate first

$$\int dz\,\bar{n}_y^*(-D^2 + F + i\bar{\omega})\,(-D^2 + G + ik\bar{\omega})\,\bar{n}_y\,.$$

This integral contains terms of the form $\int dz\,\bar{n}_y^*\,D^4\,\bar{n}_y$ and $\int dz\,\bar{n}_y^*(-D^2\,\bar{n}_y)$ which we integrate by parts taking into account boundary conditions at $z = \pm 1 : \bar{n}_y = 0$ and from eq. (4.2) $D^2\,\bar{n}_y = 0$ (with $\bar{n}_z = 0$).

Consider then the term $\int dz\,\sigma E_r\,\bar{n}_y^*\,D\bar{v}_x$. Through an integration by parts and the condition $\bar{v}_x = 0$ at $z = \pm 1$ using eq. (4.3) one gets :

$$\int dz\,\sigma E_r\,\bar{n}_y^*\,D\bar{v}_x = -\int dz\,\sigma\bar{v}_x\,E_r\,D\bar{n}_y^* = \frac{\sigma}{e-1}\left[\int dz\,\bar{v}_x(-D^2\,\bar{v}_x^*) + i\sigma\varepsilon\bar{\omega}\int dz\,\bar{v}_x\,D\bar{n}_z^*\right].$$

Again we have

$$\int dz\,\bar{v}_x(-D^2\,\bar{v}_x^*) = \int dz\,|\,D\bar{v}_x\,|^2$$

and using (4.1) we deduce :

$$\int dz\,\bar{v}_x\,D\bar{n}_z^* = -\int dz\,\bar{n}_x^*\,D\bar{v}_x = \int dz\,\bar{n}_z^*\,[E_r\,\bar{n}_y + \sigma(-D^2 + F + i\bar{\omega})\,\bar{n}_z] = \\ = \sigma\left[\int dz\,|\,D\bar{n}_z\,|^2 + (F + i\bar{\omega})\int dz\,|\,\bar{n}_z\,|^2\right] + \int dz\,\bar{n}_y\,E_r\,\bar{n}_z^*\,.$$

Finally from eq. (4.2) :

$$\int dz\,\bar{n}_y\,E_r\,\bar{n}_z^* = \int dz\,\bar{n}_y(-D^2 + G - ik\bar{\omega})\,\bar{n}_z^* = \int dz\,|\,D\bar{n}_y\,|^2 + (G - ik\bar{\omega})\int dz\,|\,\bar{n}_y\,|^2\,.$$

Eq. (B.1) now reads :

$$\int dz \mid D^2 \bar{n}_y \mid^2 + \left[F + G + i\bar{\omega}\left(1 + k + \frac{\varepsilon}{e-1}\right)\right] \int dz \mid D\bar{n}_y \mid^2 + \left[(F + i\bar{\omega})(G + ik\bar{\omega}) + \frac{i\bar{\omega}\varepsilon}{e-1}(G - ik\bar{\omega}) + \sigma E_r^2\right] \int dz \mid \bar{n}_y \mid^2 + \frac{\sigma}{e-1} \int dz \mid D\bar{v}_x \mid^2 + \frac{i\sigma\varepsilon\bar{\omega}}{e-1} \int dz \mid D\bar{n}_z \mid^2 + (F + i\bar{\omega}) \int dz \mid \bar{n}_z \mid^2 . \quad (B.2)$$

The real and imaginary part of this equation must vanish separately. In particular the imaginary part reads :

$$i\bar{\omega}\left\{\left(1 + k + \frac{\varepsilon}{e-1}\right) \int dz \mid D\bar{n}_y \mid^2 + \left[kF + G\left(1 + \frac{\varepsilon}{e-1}\right)\right] \int dz \mid \bar{n}_y \mid^2 + \frac{\sigma\varepsilon}{e-1}\left[\int dz \mid D\bar{n}_z \mid^2 + F \int dz \mid \bar{n}_z \mid^2\right]\right\} = 0 . \quad (B.3)$$

In most samples α_3 is very small and terms in ε may be neglected in eq. (B.3) (typical value in MBBA is $\varepsilon = \alpha_3^2/\gamma_1 \eta_1 \simeq 8 \times 10^{-4}$) which reduces to :

$$i\bar{\omega}\left\{(1 + k) \int dz \mid D\bar{n}_y \mid^2 + (G + kF) \int dz \mid \bar{n}_y \mid^2\right\} = 0 .$$

The quantity in brackets is always positive in the distorted state, this implies that the instability is stationnary ($\bar{\omega} = 0$). The condition :

$$\int dz \mid D^2 \bar{n}_y \mid^2 + (F + G) \int dz \mid D\bar{n}_y \mid^2 + (FG + \sigma E_r^2) \int dz \mid \bar{n}_y \mid^2 + \frac{\sigma}{e-1} \int dz \mid D\bar{v}_x \mid^2 = 0$$

in the real part of eq. (B.2) leads to a non-trivial solution only when $\sigma = -1$ or $\alpha_3 < 0$, i.e. when the mechanism described in section 3.1 is truly destabilizing.

References and Notes

[1] GUYON, E., PIERANSKI, P., *Physica* **73** (1974) 184.
Other general references will soon become available :
a) GUYON, E., Lecture notes, *NATO Advanced Study Institute*, Geilo (1975) to be published by Plenum Press.
b) DUBOIS-VIOLETTE, E., DURAND, G., GUYON, E., MANNEVILLE, P., PIERANSKI, P., to be published as a chapter of a *Supplement to Solid State Phys.*

[2] PIERANSKI, P., GUYON, E., *Solid State Commun.* **13** (1973) 435.

[3] PIERANSKI, P., GUYON, E., *Phys. Rev. A* **9** (1974) 404.

[4] Orsay Liquid Crystal Group, *Mol. Cryst. Liq. Cryst.* **12** (1971) 251.

[5] GUYON, E., PIERANSKI, P., *J. Physique Colloq.* **36** (1975) C 1-203.

[6] CHANDRASEKHAR, S., *Hydrodynamic and Hydromagnetic Stability* (Clarendon Press, Oxford) 1961.

[7] PENZ, P. A., *Phys. Rev. A* **10** (1974) 1300.

[8] PIKIN, S. A., SHTOL'BERG, A. A., *Kristallografiya* **18** (1973) 445, *Sov. Phys. Crystallogr.* **18** (1973) 283.

[9] DUBOIS-VIOLETTE, E., *Solid State Commun.* **14** (1974) 767.

[10] DUBOIS-VIOLETTE, E., *J. Physique* **33** (1972) 95.

[11] For a Review see :
a) DE GENNES, P. G., *The Physics of Liquid Crystals* (Clarendon Press, Oxford) 1974.
b) STEPHEN, M. J., STRALEY, J. P., *Rev. Mod. Phys.* **46** (1974) 617.

[12] In order to characterize a flow one usually chooses the Reynolds number $R = va/\nu = sa^2 \rho/\eta$. R may be understood as the ratio of the time scale for the diffusion of velocity to the time scale for convective transport $t_c = a/v = 1/s$. In our problem, due to the coupling between flow and molecular orientation, one can define an Ericksen number (see ref. [11a]) which compares the diffusion of orientation to convective transport

$$E_r = t_0/t_c = sa^2 \gamma/K .$$

The ratio $R/E_r = t_v/t_0$ is typically 10^{-4}-10^{-6} which explains why instabilities appear at very low Reynolds numbers. This is similar to the Rayleigh Bénard instability where in terms of conventional Rayleigh numbers the threshold is much smaller in N.L.C. than in isotropic liquids.
DUBOIS-VIOLETTE, E., C.R., *Hebd. Séan. Acad. Sci. B* **273** (1971) 923.

[13] α_2 and α_3 have to fulfil the thermodynamic inequality

$$\gamma_1 = \alpha_3 - \alpha_2 > 0 .$$

Since for geometrical reasons $\mid \alpha_2 \mid \gg \mid \alpha_3 \mid$ we must have $\alpha_2 < 0$ but α_3 may be negative (case of MBBA) as well as positive (case of HBAB at 80 °C);
a) GÄHWILLER, Ch., *Mol. Cryst. Liq. Cryst.* **10** (1973) 301.
b) PIERANSKI, P., GUYON, E., *Phys. Rev. Lett.* **32** (1974) 924.

[14] When $\alpha_3 > 0$ (or $\sigma = +1$) a homogeneous distortion cannot appear as long as the applied fields are stabilizing. However if $\varepsilon_a > 0$ the electric field is destabilizing and a *Fredericks transition* [11] takes place at a threshold field function of the applied shear.

[15] It is easy to check that $E'^2 = FG$ is a solution of eq. (4.5-4.6) but one then shows that, in general, this solution is the trivial one $n_y = n_z = v_x = 0$ everywhere.

[16] DIGUET, D., RONDELEZ, F., DURAND, G., *C. R. Hebd. Séan. Acad. Sci.* Paris *B* **271** (1970) 954.

[17] GASPAROUX, H., REGAYA, B., PROST, J., *C. R. Hebd. Séan. Acad. Sci.* Paris *B* **272** (1971) 1168. Values are given in CGS/g, calculations have been performed with

$$\chi_a = 1.24 \times 10^{-7} \text{ CGS/cm}^3 .$$